Proceedings of the ASME 2017 International Design Engineering Technical Conferences and Computers and Information in Engineering Conference
IDETC/CIE 2017
August 6-9, 2017, Cleveland, Ohio, USA

DETC2017-67436

DESIGN OF A MULTI-DIRECTIONAL HYBRID-LOCOMOTION MODULAR ROBOT WITH FEEDFORWARD STABILITY CONTROL

Prashant Kumar
Robotics and Mechatronics Lab
Dept. of Mechanical Engineering
Virginia Tech
Blacksburg, VA, USA
pkr@vt.edu

Wael Saab
Robotics and Mechatronics Lab
Dept. of Mechanical Engineering
Virginia Tech
Blacksburg, VA, USA
waelsaab@vt.edu

Pinhas Ben-Tzvi
Robotics and Mechatronics Lab
Dept. of Mechanical Engineering
Virginia Tech
Blacksburg, VA, USA
bentzvi@vt.edu

ABSTRACT

This paper presents the design of a modular robot capable of multi-directional mobility to aid reconfiguration on uneven terrain. Modular reconfigurable robotic systems consist of a large number of self-sufficient modules that can dock and reconfigure to scale locomotion and manipulation capabilities. However, on uneven terrains, reconfigurable robots face challenges due to the requirement of precise alignment between modules during the docking procedure. First, a survey of current modular reconfigurable robots is presented, analyzing their strengths and shortcomings in reconfiguration and mobility. A novel design is formulated that features a hybrid combination of wheels and tracks, symmetrically assembled about the front and right planes, providing multi-directional mobility and modularity. The robot can move over uneven terrain via tracks, move at higher speeds via wheels placed orthogonally to the tracks, and move in the vertical direction via a vertical translation mechanism in order to aid in multi-robot docking. Both the wheels and tracks possess yaw mobility via differential drive. The design's compact size and hybrid multi-directional mobility system make the robot highly mobile on uneven terrain. Presented in this paper are the mechanical and electrical design and a feedforward dynamic stability controller, the performance of which is validated using a simulated case study.

NOMENCLATURE

m_{TU}	Mass of Tracked Unit (TU)
m_{VTU}	Mass of Vertical Translation Unit (VTU)
m_{WU}	Mass of Wheeled Unit (WU)
m_{Other}	Mass of Support Rods and other components
m	Mass of Robot
z_{VTU}	Translation of VTU
cm	Center of Mass (CM) of Robot
cm_{TU}	CM of TU
cm_{VWU}	CM of VTU and WU
h_{CM}	Height of CM of Robot
h_{VWU}	Height of CM of VTU and WU
h_{TU}	Height of CM of TU
b_{TU}	Horizontal distance of cm_{TU} from cm
P	Point of contact of shown wheel to ground
b_{WU}	Horizontal distance of P from cm
r_W	Radius of wheel of robot
a	Acceleration of robot along positive Y'-axis
β	Angle of slope
S	Center of wheel of robot
O_i	Coordinate of CM of robot in initial position
O_t	Coordinate of CM of robot in toppling position
O	Coordinate of CM of robot
O_Y	Y Coordinate of O
O_Z	Z Coordinate of O
θ	Angle of rotation of robot
θ_t	Angle to rotate robot to make it topple
θ_f	Angle robot allowed to rotate by controller
ω_o	Initial angular velocity of robot along x-axis through S
ω_{topple}	Angular velocity to topple robot along x-axis through S
h_{topple}	Height robot needs to climb to topple
I_S	Moment of inertia of robot along x-axis through S
α_θ	Angular acceleration of robot varying with θ
F_μ	Frictional force at wheel and ground contact

1. INTRODUCTION

Rigid structure robots are typically designed to perform a single, specialized task in a repeatable manner. Engineers can ensure ideal operating conditions with near certainty. However,

these robots face challenges when tasks and terrain are undefined. In such cases, it would be beneficial for the robot to be capable of adapting by forming new configurations to enable new functionalities. These challenges have driven research in the field of modular reconfigurable robotics.

Modular reconfigurable robots consist of several self-sufficient modules capable of sensing, processing and actuation. Modules can reconfigure, a process in which discrete modules dock (connect) to each other to scale locomotion and manipulation capabilities [1]. These characteristics make modular robots more versatile and robust with lower unit production costs compared to a high-capability rigid structured robot [2]. However, the advantages of modular reconfigurable robots have not yet been fully realized due in part to challenges of reconfiguration on uneven terrain [3]. The main technical challenge is precisely aligning two modules within a certain tolerance to ensure successful docking. Uneven terrain increases the misalignment manifold that must be compensated for and task becomes increasing difficult if the robot is limited in its directional mobility.

In this paper, we discuss the current designs of modular reconfigurable robots along with challenges in the mobility domain, to arrive at a desired set of characteristics of a modular reconfigurable mobile robot. To address these challenges and desired characteristics, we present a novel design of a multi-directional hybrid-locomotion modular robot to aid reconfiguration on un-even terrain. The long-term goal of this research is to design highly mobile modular self-reconfigurable robots capable of self-reconfiguring on uneven terrain to scale manipulation and locomotion capabilities [1], [4]–[6].

This paper is organized as follows: Sec. 2 classifies the locomotion type of current modular reconfigurable robots and the mobility systems employed by these robots. Section 3 discusses about strengths and shortcomings of mobility systems for different applications and proposes design characteristics desired for the mobility system for the application under consideration, as well as details the robot design. Section 4 is an overview of the electronics of the design. Section 5 analyzes the stability of the design. Section 6 presents a feedforward control model for dynamic stability of the robot. Section 7 presents the simulation results of the control model. Lastly, Sec. 8 describes the conclusion and future work of our research.

2. BACKGROUND

This section reviews the field of modular reconfigurable robots in Sec. 2.1, and the mobility systems employed in these and other mobile robots in Sec. 2.2.

2.1 Modular Reconfigurable Robots

Modular and reconfigurable robots are classified into two major categories: Mobile Configuration Change (MCC) and Whole Body Locomotion (WBL) [7]. These categories are differentiated by their mobility patterns and the reconfigurable properties of the robot.

MCC refers to modular robots where individual modules physically connect to one another to change the group configuration and augment the capabilities of a single module.

Table 1. Pre-configuration State Locomotion Type and Mobility Systems of Modular Reconfigurable Robots.

Robot Name	Pre-configuration Locomotion Type	Mobility System
S-Bots [14]	MCC	Track, Wheel
JL-I&II Robot [9][15]	MCC	Track
Millibots [16]	MCC	Track
AMOEBA [17]	MCC	Track
Tetrobot [18]	MCC	Roll, Leg
iMobot [19]	MCC	Crawl, Roll, Leg
PolyBot [20]	WBL	Roll, Leg
GZ-I Robot [21]	WBL	Leg
CKBot [11]	WBL	Roll, Leg
OCTABOT [22]	WBL	-
Odin [23]	WBL	Spatial Contractions
I-Cubes [24]	WBL	Leg
Roombots [25]	WBL	Roll, Leg
Molecubes [26]	WBL	Roll
Uni-Rover [27]	WBL	Wheel
CONRO [28]	WBL	Roll, Leg

This generally takes the form of a head-to-tail docking process but can exhibit other topologies. In this category, individual modules are self-contained and possess sufficient sensing, computing and actuating capabilities to operate individually.

WBL relates to modular robots whose morphology can provide different types of locomotion, such as walking, crawling and rolling. This is generally achieved by reconfiguring the degrees of freedom (DOF) and controlling the joints in order to reshape the structure into a desired configuration. The docking patterns with WBL can be realized in architectures including chain [8][9], lattice [10][11] and hybrid chain-lattice [12][13]. The main difference between WBL and MCC is that the modules in WBL can only provide useful mobility when connected together via docking interfaces. In contrast, MCC modules are independent entities capable of achieving individual mobility even in the undocked configuration. Table 1 presents a selection of modular reconfigurable robots and classifies them according to their pre-configuration state locomotion type and mobility system. Important design features of the listed robots are discussed.

S-Bots are autonomous robots employing track locomotion. They connect together in train like formation to do swarm robotics applications [14]. JL-1 and JL-2 are trapezoidal tank like tracked MCC robots [15][9]. Millibots are tacked robots with individual mobility, forming train like configurations [16]. AMOEBA is tracked robot with one track covering the whole body. It is able to move only in one direction without the capability to change direction on its own. On docking with other modules, it can implement differential drive to make turns [17]. Tetrobot is a truss shaped robot, which can do locomotion by changing shape or move about slowly by employing a few of its links for legged mobility [18]. Each module of iMobot has four degrees of freedom that can crawl, lift itself and attach to others to form larger shapes [19].

Table 2: Comparison of major locomotion systems in robots.

Feature \ Locomotion	Offered Speed	Obstacle Traversal	Gravel/ Soft Ground Traversal	Slope/ Plank Traversal	Mechanical Complexity	Offered Positional Control	Energy Efficiency	Load Carrying Capacity
Conventional Wheeled	High	Low	Low	Medium	Low	Medium	High	Medium
Tracked	Medium	Medium	High	High	Low	High	Medium	High
Legged	Low	High	Low	Low	High	Low	Low	Low
Roll (Whole Body)	Low	Low	Low	Low	High	Low	Low	Low
Omni-Dir. Wheel	Low	Low	Low	Low	Medium	Low	Medium	Low
Hybrid	Low	Varies	Varies	Varies	High	Low	Low	Low

Polybot is collection of cube like modules, which exhibit little individual mobility but can connect together in snake/chain like formations to do larger tasks [20]. GZ-I Robot is a WBL, with each module having a rotation degree of freedom perpendicular to the body of the module [21]. Its modules do not have locomotion capability. CKBot is a chain based WBL modular reconfigurable robot with each module in shape of cube. The main aim of CKBot was to show reconfigurability rather than locomotion [11]. OCTABOT is a WBL in which individual modules do not have their own mobility system but use electromagnets to attract other modules and reconfigure [22]. Odin is a truss shaped WBL robot where each link can change length [23]. I-Cubes is a WBL robot made of two types of elements: an active element capable of actuation and a passive element that connects two active elements [24]. This combination can traverse obstacles via legged locomotion. Roombots are cube shaped WBL robots that can actuate about a plane to form different shapes of furniture [25]. Molecubes are cube shaped modules, which can rotate about a plane and dock together to form linear or larger shapes, with the aim to be adopted as a standardized modular reconfigurable research platform [26]. Uni-rover, classified as WBL, has smaller modules that function like wheels when connected together to a separate main body [27]. CONRO is WBL type modular robot, which can configure into different shapes and do locomotion by roll or legged motion [28].

In this preceding paragraph, we classified modular reconfigurable robots based on their pre-configuration locomotion capacity. As discussed, many reconfigurable robots are WBL in nature while for our application we will focus on MCC type modular reconfigurable robots.

2.2 Mobility Systems

This section compares the most common types of locomotion systems and provides a comparison based on speed, performance on various terrains, mechanical complexity, control, energy efficiency and load carrying capacity.

Modern field robotic technology is dominated by two main mobility systems: wheels and tracks. Wheels can be cylindrical, spherical, omni-directional [29], [30]. In field applications, the selection of a specific mobility system is contingent on the terrain where the robot is expected to operate. On flat surfaces wheeled locomotion performs better for most operations. Because of less ground-contact wheels experience low friction which promotes fast maneuverability and low power consumption. On rugged terrains and soft terrains, like mud and sand, tracks are more efficient. Here the robot's weight gets distributed over a larger area with the ground. Though, for field applications however, neither of these two terrains are constantly present. Instead, a hybrid blend of both terrains forms a surface where neither wheels nor tracks alone can optimal mobility. Such a limitation has spurred research in a new generation of mobile robots that can adapt their locomotion pattern with changing terrain. The most common of these are robots that combine wheels and tracks in a single platform. Many such robots consist of two timing belts wrapped around pulleys, with the possibility of manually attaching four eccentric wheels each on the every pulley, to switch to wheel-based mobility [31].

A more automated version of such an implementation employs a mechanism that toggles between wheels and tracks [32], [33] with the possibility of integrating belt-driven front and back flippers [34] to enable legged locomotion for military applications. Additional variations include articulated wheels that can be reconfigure into legs [35], [36], and articulated tracks [37] that can reshape into wheels. New ideas have been shown in using track wheel combination for application like mobility assistive devices, such as wheelchairs [38].

The majority of current hybrid mobility designs are capable of longitudinal motion with differential steering, with no potential for lateral or omni-directional mobility [34]. On unstructured terrains and crowded environments, additional degree of freedoms like lateral or omni-directional mobility significantly improve their maneuverability [10], [39]–[45].

We compare the major locomotion systems employed by modular reconfigurable robots in Sec. 2.1, based on speed, performance in different terrains, mechanical complexity, positional control, energy efficiency and load carrying capacity in Table 2. The typical systems are Conventional Wheels, Tracks and Legs. Many WBL robots move by rolling of their whole body, which is also compared. Another popular locomotion system used is Omni-Directional Wheels like Castor Wheel, Universal Wheel, Mecanum Wheel and Ball Wheel Mechanism [46]. Hybrid systems are a combination of multiple systems, e.g. an actuation unit toggles its shape between wheels or legs as required, such as [47].

Wheeled systems provide high speeds, low complexity and medium positional control but low performance in uneven terrain like soft ground and obstacles. Tracked systems provide good performance in uneven terrain but have lower speeds.

Table 3. Comparison of degrees of freedom and design complexity in some popular rigid-structured robots.

Robot \ Deg. of Freedom	Mobility System	X	Y	Z	Yaw	Roll	Pitch
SR2 Rover [49]	Wheel	✓			✓		
Micro5 Rover [50]	Wheel	✓			✓		
PackBot [51]	Track	✓		✓	✓		✓
Seegrid Trucks [52]	Wheel	✓		✓			
RHex [53]	Leg	✓			✓		
BigDog [54]	Leg	✓	✓	✓	✓		
Azimut [55]	Track, Leg	✓	✓	✓	✓		✓

Legged and hybrid systems are complex designs offering lower control. Roll offers lower levels of mobility and control. Omni-directional wheeled systems have lower performance in uneven terrain as well as offer lower control [46]. From this comparison, we see that Wheeled and Tracked systems complement each other's shortcomings. A hybrid robot using both would likely be able to traverse in even and uneven terrains well, with high speed when possible and offer good positional control with lower complexity.

Table 3 provides a comparison of degrees of freedom in some popular single-structured robots. We see that most tracked and wheeled system robots have low mobility complexity but have mobility only in longitudinal direction not lateral direction. While most legged robots provide mobility in both longitudinal and lateral directions, they have higher mobility complexity. Higher mobility complexity reduces control as well as speed.

3. DESIGN APPROACH AND OVERVIEW

3.1 Design Approach

In the effort to improve the modularity, mobility, and reconfigurability, based on the discussions in Sec. 2, we detail the following as the design requirements for an idealized modular robotic system:

- *Modularity:* A single module should be composed of similar sub-assemblies to fully realize the advantages of modularity in a single and multi-robot configuration.
- *Mobility:* A modular robot should be capable of spatial mobility, i.e., six DOF, three translational in X, Y, Z and three rotational in roll, pitch and yaw. Multi-directional mobility will aid in reconfiguration on uneven terrain.
- *Reconfigurability:* The design should have one or more high strength, rigid docking points capable of tolerating misalignments about six spatial directions

The goal in this paper is to design a modular reconfigurable robotic platform. Therefore, we focus our efforts in realizing modularity and mobility in the proposed design. The reconfigurability requirement will be left for future work by adding highly capable docking interfaces developed by the authors [1][5][48][57].

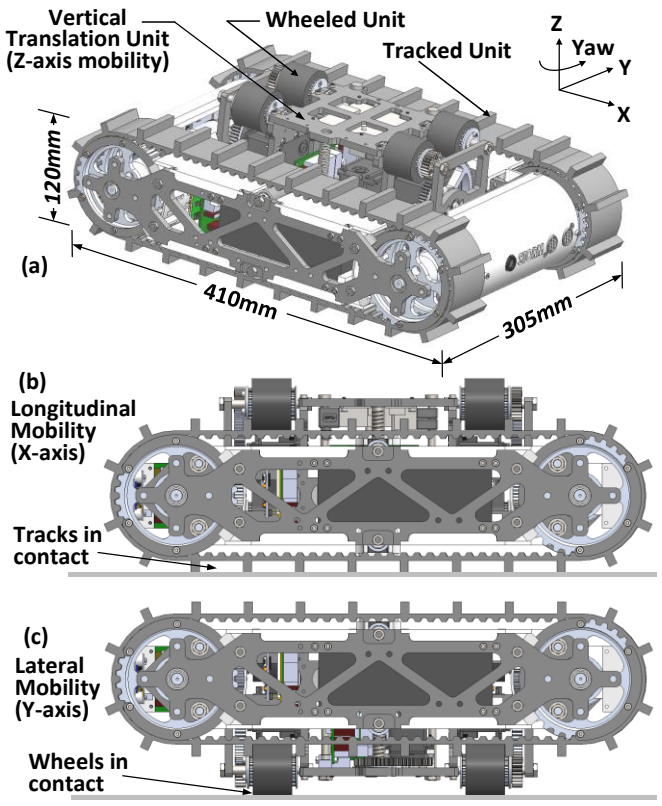

Figure 1. A CAD model of the proposed hybrid mobility robot (a) showing the perspective view, (b) showing Tracks in contact with ground and (c) showing wheels along Y-axis in contact with ground [56].

3.2 Design Overview

The proposed hybrid mobility robot [56] has the capability to move in longitudinally on tracks, laterally on wheels, translation in vertical direction and yaw differentially along the vertical direction on both wheels as well as tracks, as shown in Fig. 1. The design consists of three main sub-assemblies: two Tracked Unit (TU), two Wheeled Unit (WU) and one Vertical Translation Unit (VTU). The TU provides forward X-axis locomotion Fig. 1(b) and VTU can be deployed to provide Y-axis locomotion and Z-axis height adjustment Fig. 1(c). Both the wheels and tracks possess yaw direction mobility via differential drive. The assembly is designed to maintain symmetry of the platform along the front (Y-Z) and right (X-Z) planes. Four support rods rigidly connect the two TUs together.

Table 4. Physical Design Parameters

Characteristic	Design Value
Outer Dimensions	410 x 305 x 120 mm^3
Vertical Translation	50 mm
Max climb angle	40°
Robot Mass	8.40 kg
TU Mass	2 x 2.81 kg
WU Mass	2 x 0.76 kg
VTU	0.73 kg

The VTU has a 3-point contact with the robot on three parallel axes of which two are passive guideways and one is an active lead screw and nut mechanism. The two WUs attach to the two sides of the VTU. This hybrid tracked/wheeled design makes the robot useful on both even and uneven terrain. The overall mass of the current implementation of this robot design, including electronics, is 8.4 kg. Table 4 presents the physical design paramters of the system.

3.2.1 Tracked Unit

The hull of the TU consists of two parallel side plates rigidly connected together using four connecting rods. It houses two pulley sets: an active pulley pair driven by a DC motor through a speed reduction gearbox, and a passive pulley pair as shown in Fig. 2.

A timing belt, which also acts as the robot's tracks, runs over these pulleys. Two passive rollers in the middle section of the TU support this timing belt. The length of the unit is 410 mm, its height is 120 mm and its width is 80 mm. The pulleys are 30-tooth T10 pulley with pitch diameter 95.49 mm supplied by Brecoflex. The timing belt is a 50 mm wide T10 tooth-profile BFX timing belt, of polyurethane material PU-385, supplied by Brecoflex, of length 920 mm with cuboidal back-profiles of cross-section 9 mm x 6.5 mm and pitch 40 mm to increase robot traction on uneven terrain. The robot ground clearance using the selected belt back-profile height of 9 mm is 16 mm. Any increase in the size of the back-profile will increase the ground clearance.

The DC motor directly drives the pulleys through a gearbox. The gearbox has radial load capacity of 240 N while the loads on the pulley are 20 N during normal operations on flat ground and 82 N if the weight of the robot is applied to a single pulley during operation. Additionally, the polyurethane tracks provides damping which reduces the impulsive loading on the gearbox [4], [6]. Caps are installed on the sides of the pulleys to hold the track on the pulley face.

The selected motor is an 18 V Maxon Motor (EC-i series 496654) with a nominal speed of 6890 rpm and nominal torque of 105 mNm. A Maxon gearbox (203116) with 15:1 gear reduction provides the robot a nominal translation speed of 3.01 m/s. The motor/gearbox combination provides a continuous nominal torque of 1.7 Nm, which is sufficient torque to traverse the robot over 30 degree inclines easily. The required torque for this traversal is 1.51 Nm with a 1.3 safety factor. Being a modular design, this motor gearbox combination can be changed as per desired requirement. This TU also houses a battery pack as shown in Fig. 2. The battery set is composed of three 14.4V 32 Wh 2.2 Ah with 4 A discharge rate Li-ion batteries (Batteryspace LCH2S4I2WR). To implement position control, a 360-step encoder (US-Digital E4T-360-236-D-H-M-B) is used which has been placed on the back of the motor. Lastly, the TU also houses a Maxon motor driver (438725) which interfaces with the motor and encoder. The Vertical Translational Unit houses the controller, detailed later.

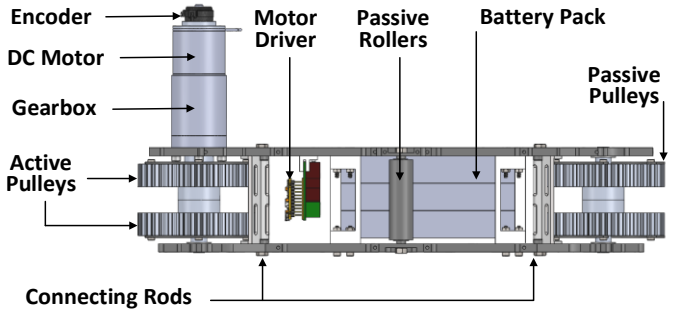

Figure 2. Top view of the TU showing the pulleys, the motor/gear-stage assembly and pertinent electrical layout.

3.2.2 Wheeled Unit

The WU consists of four rubber wheels: two active and two passive, two gears to run the active wheels called roller gears, a driving gear to transfer power to the roller gears and a continuous servomotor to actuate the driving gear as shown in Fig. 3(a). Additionally, to increase flexibility of the design, four pulleys are used instead of a cylindrical shaft to mount the wheels. This gives the operator the freedom to mount tracks or wheels on the WU based on the required application as shown in Fig. 3(b).

The driving gear is an 80-tooth module-1 gear with pitch diameter 80 mm. The roller gear is a 24-tooth module-1 gear with pitch diameter 24 mm. Adding the pitch radius of both the gears gives the length of AO and BO, as shown in Fig. 3, which is 52 mm. The pulleys rotate on a stationary shaft using two bearings each. As shown in Fig. 3, two are active while two are passive. The pulley chosen is 16-tooth T5 pulley with pitch diameter 25.46 mm and face width of 35 mm supplied by Brecoflex, Two removable flanges at either end keep rubber wheel or timing belt cum track on the pulley face. The rubber wheels are 30 mm wide and 40 mm in diameter. The timing belt is 30 mm wide T5 tooth-profile BFX timing belt of polyurethane material PU-385 supplied by Brecoflex of length 400 mm with cuboidal profiles of cross-section 6 mm x 4 mm and pitch 20 mm on back to increase robot traction in uneven terrain. The VTU houses the controller of this unit and is described in Sec. 3.2.3.

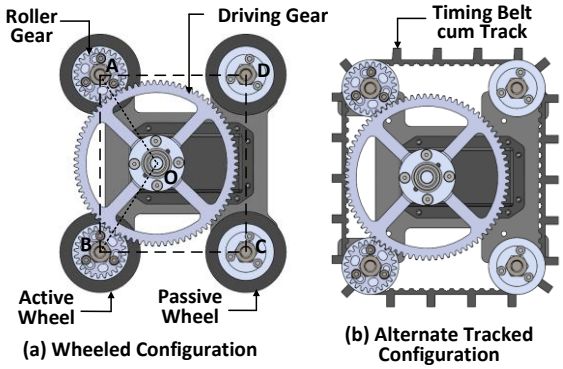

Figure 3. (a) CAD Model of the WU showing the gear-pulley-wheel assembly. (b) alternative configuration using tracks instead of wheels.

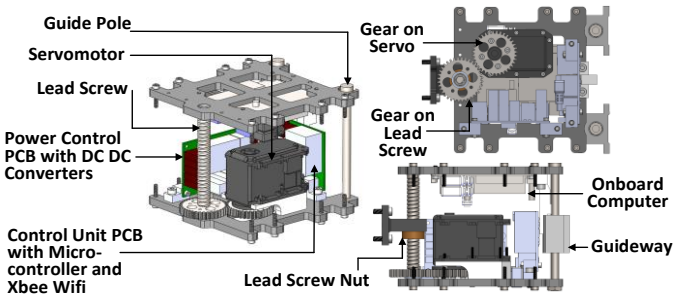

Figure 4. CAD Model of the VTU showing leadscrew and nut assembly as well as all electronics.

3.2.3 Vertical Translational Unit

The VTU provides relative translation along the vertical Z-axis between the wheeled and TUs. VTU's translation is actuated by a lead screw and nut mechanism driven by a servomotor and two spur gears as shown in Fig. 4. The lead screw and nut assembly (Powerac Trapezoidal Assembly 900 RS with Bronze Nut) is non-back-drivable and provides self-locking action removing the need for an additional locking mechanism to lock the VTU at a specified height. A Dynamixel MX-64R servomotor is used. The two spur gears are 36-tooth module-1 gears with pitch diameter 36 mm. The lead screw and nut mechanism provides a translation of 25 mm in vertical direction whereas required translation is 20 mm to reach maximum ground clearance of 16 mm. Since the gears used in the VTU are equal in pitch diameter, the lead screw rotates at the servomotor's rotation speed. The lead screw pitch is 1.5 mm; therefore, for one complete rotation of the lead screw, the lead screw nut will translate the VTU by 1.5 mm.

The VTU makes a three-point contact with the robot: one at the lead screw and nut assembly and two at guide pole and guideway assemblies shown in Fig. 4. The guide poles are quarter inch thick and translate freely along the vertical direction on two guideways – mounted linear sleeve bearings sourced from McMaster (6374K115).

The VTU houses the custom Control Unit PCB with a microcontroller (Teensy 3.2) and an XBee WiFi communication module, the Power Control PCB made in lab and a commercial on-board computer ODROID XU4.

4. ELECTRONICS DESIGN

The proposed electrical design of the robot, as shown in Fig. 5, is divided into two sections: Actuation Schematics and Sensing Schematics. From the six batteries in the two TUs three series pairs are made which are then connected in parallel, providing a voltage of 28.8 V and max discharge rate of 12 A overall. The battery pack directly powers the Motor Drivers. A Teensy 3.2 microcontroller provides control signals to the two motor drivers for the two TU's DC motors and the three servomotors, two of which are in the WUs and one in the VTU. It also reads inputs from an accelerometer cum gyroscope cum magnetometer IMU. An ODROID XU4 onboard computer and the Teensy 3.2 Microcontroller are used for sensing and

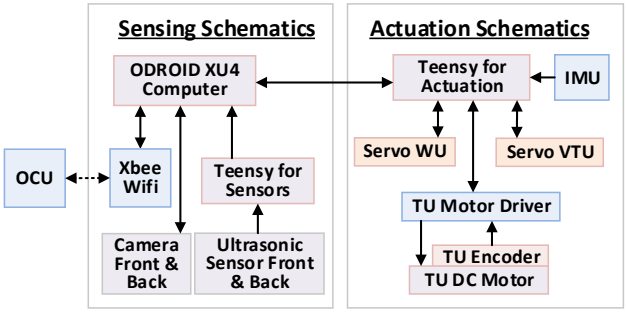

Figure 5. Electronic schematic of robot.

communication. Two Ultrasonic distance sensors are put in front and back of the robot. Additionally, two 5MP USB cameras will be used for image processing. An Xbee WiFi module is used for wireless communication with operator control unit (OCU).

5. STABILITY ANALYSIS

During tracked locomotion, the system is inherently stable since the tracks are relatively wide apart and support the full length of the robot. However, wheeled locomotion is prone to instability, toppling, since the wheels have a shorter support region and operate when the TU is lifted off the ground. In this section we analyze the stability requirements of wheeled locomotion. In reference to Fig. 1, when the wheeled units are in contact with the ground the support polygon measures 193 mm along the X-axis and 72.4 mm along the Y-axis. This distance is relatively small compared to the 305 mm width of the robot and could cause toppling during wheeled locomotion. Stability analysis will involve computing the maximum accelerations and ground incline angle capable to prevent the robot from tipping over.

Figure 6 shows a simplified free body diagram (side view) of the robot's side view while during wheeled locomotion on a plane inclined at an angle β. The CM of the robot can be calculated using the following relation

$$h_{cm} = \frac{(2m_{TU} + m_{Other})h_{TU} + (m_{VTU} + 2m_{WU})h_{VWU}}{2m_{TU} + m_{Other} + m_{VTU} + 2m_{WU}} \quad (1)$$

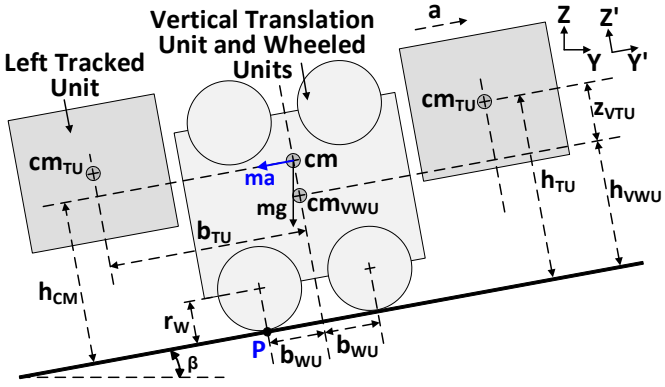

Figure 6. Wheeled locomotion free body diagram (Y-Z plane of design).

During high accelerations, toppling may occur about point P which is the point of contact of rear wheel with ground when balance of torques shifts to counter-clockwise direction. Because of acceleration *a* of robot along Y' axis, the robot will experience a pseudo force *-ma* as shown. To maintain stability, a balance of torques about point P yields

$$a < \frac{b_{WU}}{h_{CM}} g\cos\beta - g\sin\beta \quad (2)$$

Equation 2 represents the relation between maximum acceleration on an incline with angle β, the robot can sustain without toppling. Table 5 presents the robot physical parameters. Using Eq. 2 the robot can accelerate at up to 4.52 m/s^2 on flat plane which non-linearly reduces to 0 m/s^2 for a maximum traversable angle of 24.7°. With this inequality, a first layer of control can be built on the operator module to not provide accelerations higher than these limits during wheeled locomotion.

6. FEED-FORWARD CONTROL MODEL FOR DYNAMIC STABILITY CONTROL

This section describes a controller to stabilize the robot during wheeled locomotion. Finding perfectly flat surface is difficult and generally, surfaces will have imperfections that may provide disturbance forces and impulses to the robot. Since the robot has a restricted stability in wheeled locomotion, a vertical impulse can create imbalance and cause it to topple. Therefore, to increase stability of the robot, we design a feed forward controller, which corrects disturbances by controlling acceleration and deceleration of the robot. This controller uses the robot's attitude, specifically the angular velocity, orientation, and linear acceleration inputs from the IMU, determines if there is an imbalance by keeping track of change in the robot's angular velocity, computes the toppling condition based on a feed forward model, and calculates required accelerations as corrections from the motor to avert toppling. This controller can work both ways to counter toppling in the forward as well as the reverse directions, by the same principle.

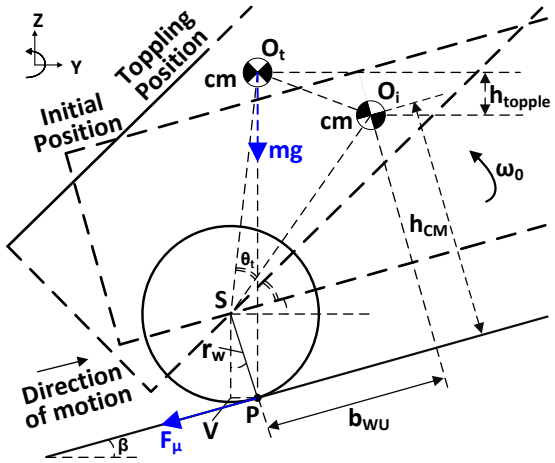

Figure 7. Free body diagram representing robot in initial position on ground with angular velocity ω_0 and toppling position where O_t is vertically above P.

The robot has the least stability to toppling along the *x*-direction of rotation. The control action provides enhanced stability to disturbances along this axis. A disturbance from the ground may be induced by an instantaneous impulse. Let's assume it is on the front wheel. Let us also assume this vertical impulse would impart an angular velocity, ω_0, to the robot in the *x*-direction about the center of rotation of the rear wheel at S, as shown in Fig. 7. Figure 7 shows a magnified cutout of the robot in two positions. The first in dashed line shows initial position when it receives this angular velocity and the second shows the toppling position, in which the center of mass of the robot O_t is directly above the point *P*. To account for the general case, calculations are done for a plank with angle β. Gravity, acting on the center of mass, provides a balancing torque to the robot to bring it back to the stable position on the ground, which is the initial position. In the limiting condition for toppling, if there is any angular velocity still left at the toppling position, the robot would topple. From Fig. 7, we see that the energy required to topple the robot from the initial position to the toppling position is equivalent to the potential energy required to shift the center of mass from O_i to O_t, which is at a height difference of h_{topple}. The coordinates of the center of mass, with *S* as the origin, when the robot is on flat ground are (b_{WU}, h_{CM}-r_W). Rotating the robot about point *S* by β, we get the coordinates of O_i:

$$\begin{bmatrix} O_{iY} \\ O_{iZ} \end{bmatrix} = \begin{bmatrix} b_{WU}cos\beta - h_{CM}sin\beta + r_W sin\beta \\ b_{WU}sin\beta + h_{CM}cos\beta - r_W cos\beta \end{bmatrix} \quad (3)$$

The coordinates of O_t, the toppling position, the robot is further rotated about point S by an angle θ_t as shown in Fig. 10. Therefore, the coordinates of O_t are:

$$\begin{bmatrix} O_{tY} \\ O_{tZ} \end{bmatrix} = \begin{bmatrix} b_{WU}cos(\beta+\theta_t) + (r_W - h_{CM})sin(\beta+\theta_t) \\ b_{WU}sin(\beta+\theta_t) - (r_W - h_{CM})cos(\beta+\theta_t) \end{bmatrix} \quad (4)$$

Since O_t is vertically above the point *P*, therefore, the Y coordinate of *P* is equal to Y coordinate of O_t. We use this condition to compute the toppling angle θ_t. The Y coordinate of point P can be computed from the triangle SVP in Fig. 8(b). Therefore, $VP=SPsin\beta=r_W sin\beta$. Equating this with the Y coordinate of O_t from Eq. 4:

$$r_W s\beta = (b_{WU}c\beta - h_{CM}s\beta + r_W s\beta)c\theta_t - (b_{WU}s\beta - h_{CM}c\beta + r_W c\beta)s\theta_t \quad (5)$$

From Eq. 5 we get the toppling angle, θ_t. From Fig. 8(b) we see h_{topple} is Z coordinate of O_t minus Z coordinate of O_i. Therefore:

$$h_{topple} = cos(\theta_t)(b_{WU}sin(\beta) + cos(\beta)(h_{CM} - r_W)) - cos(\beta)(h_{CM} - r_W) - b_{WU}sin(\beta) + sin(\theta_t)(b_{WU}cos(\beta) - sin(\beta)(h_{CM} - r_W)) \quad (6)$$

Condition of toppling is when kinetic energy of angular motion of the robot about point S is greater than the potential energy required to raise the robot by height h_{topple}, or $KE_{topple} \geq PE_{h\_topple}$:

$$\frac{1}{2} I_S \omega_{topple}^2 \geq mgh_{topple}$$

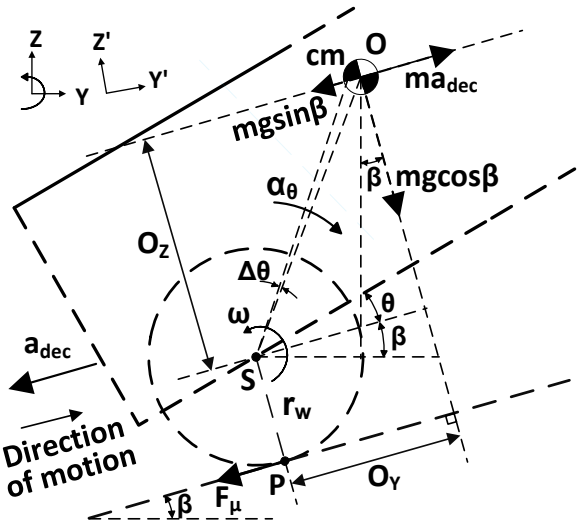

Figure 8. Simplified free body diagram (Y-Z plane) of robot during wheeled locomotion.

$$\omega_{topple} \geq \sqrt{\frac{2mgh_{topple}}{I_S}} \tag{7}$$

where I_S is the moment of inertia of the robot about the axis of rotation of the wheel through the point S.

As found in Eq. 7, if ω_0, which is the initial angular velocity, is greater than or equal to ω_{topple}, the robot will topple. We use this derivation to make a controller which will act if ω_0 is 85% or greater than ω_{topple}. The control action here would be to reduce the forward speed of the robot to provide a counter torque using friction and deceleration, creating a pseudo force, to pull the robot back towards the ground, as shown by F_μ and ma_dec, respectively, in Fig. 8. The frictional force is assumed to be rolling friction. Resolving forces along Y' direction, we see that F_μ increases from 0 with deceleration a_{dec}, with an upper limit of μmg, where μ is the friction constant. The deceleration will provide a pseudo force in the forward direction varying with the angle of the robot, θ. This pseudo force will act on the center of mass.

We use conservation of energy to derive a relation between initial angular velocity and required deceleration. We use:

$$-\Delta KE = \Delta PE + W(Workdone\ by\ ma_{dec}\ and\ F_\mu) \tag{8}$$

Workdone by ma_{dec} and F_μ can be found by resolving torques about S and finding the angular acceleration provided by these forces:

$$I_S\alpha_\theta = F_\mu r_w + ma_{dec}O_Z \tag{9}$$

Substituting O_Z in Eq. 9, we find α_θ varies with the robot pitch angle θ. To get workdone we integrate workdone by α_θ over small $\Delta\theta$ increments by using summing $I_S\alpha_\theta\Delta\theta$ over θ varying from 0 to θ_f (theta final). Assuming $\Delta\theta$ to be very small, there will be tending to infinity number of $\Delta\theta$. Using this assumption, we change summation to integral and get workdone:

$$W = \sum_{i=1}^{n\to\infty} I_S\alpha_\theta\Delta\theta = \int_{\theta=0}^{\theta=\theta_f} I_S\alpha_\theta\, d\theta \tag{10}$$

Substituting result of Eq. 10 in Eq. 8, where $-\Delta KE$ is $\frac{1}{2}I_S\omega_0^2$ and ΔPE is mgh_{climb}, where h_{climb} is the allowed climb of the robot, which we get by using θ_f as the allowed rotation, we get the required deceleration:

$$a_{dec}^{F\mu linear} = \frac{\frac{I_S\omega_0^2}{2m}+g\begin{bmatrix} b_{WU}s\beta+c\beta(h_{CM}-r_W) \\ -c\theta_f\{b_{WU}s\beta+c\beta(h_{CM}-r_W)\} \\ -s\theta_f\{b_{WU}c\beta-s\beta(h_{CM}-r_W)\}\end{bmatrix}}{\begin{matrix} r_W\theta_f-b_{WU}cos(\beta+\theta_f)+h_{CM}\sin(\beta+\theta_f) \\ -r_W sin(\beta+\theta_f)+b_{WU}c\beta-h_{CM}s\beta+r_W s\beta\end{matrix}} \tag{11}$$

$$a_{dec}^{F\mu max} = \frac{-\frac{I_S\omega_0^2}{2m}+g\begin{bmatrix} \mu r_W\theta_f c\beta-b_{WU}s\beta-c\beta(h_{CM}-r_W) \\ +c\theta_f\{b_{WU}s\beta+c\beta(h_{CM}-r_W)\} \\ +s\theta_f\{b_{WU}c\beta-s\beta(h_{CM}-r_W)\}\end{bmatrix}}{\begin{matrix} b_{WU}\cos(\beta+\theta_f)-h_{CM}\sin(\beta+\theta_f) \\ +r_W sin(\beta+\theta_f)-b_{WU}c\beta+h_{CM}s\beta-r_W s\beta\end{matrix}} \tag{12}$$

where Eq. 11 is a_{dec} when the required control action does not make $F\mu$ go to its max value of $\mu mgcos\beta$ while Eq. 12 is a_{dec} when $F\mu$ is at max value of $\mu mgcos\beta$. In the feed forward control, we set the max allowable value of θ_f as 85% of θ_t. With this control, the robot stabilizes itself using the required deceleration. The same model can be used to stabilize robot in forward direction toppling also. The effectiveness of this controller is tested in Sec. 7.

7. SIMULATION RESULTS

This section simulates case scenarios to test the effectiveness of the feedforward control model. The robot is simulated to traverse an inclined plane during wheeled locomotion, where it receives an impulse which induces a

Table 5. Simulation Design Parameters

Variable	Value	Variable	Value
m	8.40 kg	h_{cm}	0.0850 m
m_{TU}	2.81 kg	r_W	0.02 m
m_{WU}	0.76 kg	b_{WU}	0.0362 m
m_{VTU}	0.73 kg	μ	0.1
m_{Other}	0.53 kg	β	15°
h_{TU}	0.0700 m	I_{XXCM}	0.0700 kg m^2
h_{VWU}	0.1275 m	I_S	0.1170 kg m^2

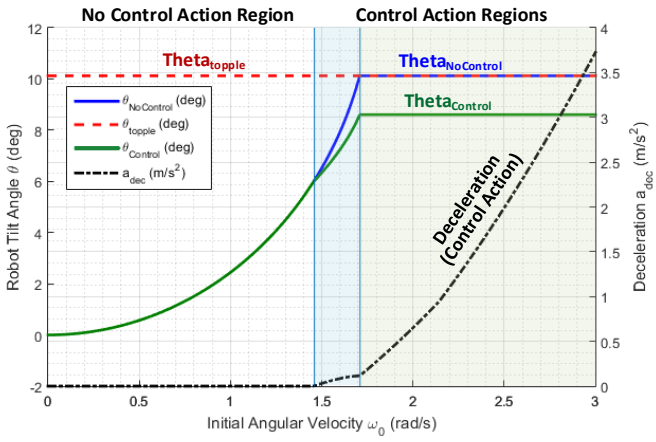

Figure 9. Simulation of control action with slope angle β = 15°.

positive angular velocity. Table 5 presents the parameters used in this simulation. The plank angle for this simulation is $\beta=15°$. Figure 9 shows the simulation results of system response for a variation of ω_0. The toppling angular velocity for this plank angle is $\omega_{topple}=1.7$ *rad/s*. Two main regions can be identified from this plot; no control action region and control action region. In the no control region, since $\omega_0 < 85\%\ \omega_{topple}$, a control action is not required since the robot is not expected to topple. The control action region has two shaded regions (blue and green). In the blue shaded region, ω_0 is between 85% and 100% of ω_{topple}. In this region although the robot is not expected to topple, the controller limits $\theta_{Control}$ to 85% of $\theta_{NoControl}$, to have additional safety against toppling. The control action is in the form of a deceleration, a_{dec}, which takes on positive non-zero values. In the green shaded region, $\omega_0 > \omega_{topple}$ the control action increases with ω_0 to limit $\theta_{Control}$ to 85% of $\theta_{NoControl}$. This simulation validates the control action of the proposed feedforward model, the performance of which depends on actuator specifications which will be further investigated in future work.

8. CONCLUSION

This paper presents a novel design of a modular reconfigurable mobile robot capable of multi directional mobility. The robot can move over uneven terrain via tracks, move at higher speeds via wheels placed orthogonally to the tracks, and move in the vertical direction via a vertical translation mechanism in order to aid in multi-robot docking. Both the wheels and tracks possess yaw mobility via differential drive. Based on stability analysis, we propose a feedforward controller and validate its performance through simulated case study.

Future work involves integrating an experimental prototype to test the robot's ability to traverse a wide variety of terrains. In addition, docking points must be designed and optimized to allow the robot to attain full reconfigurability. Finally, sensing and localization strategies must be developed then validated first with alignment algorithms that simulate the docking procedure on uneven terrain and then on a working prototype.

ACKNOWLEDGMENTS

The authors would like to acknowledge members of the Robotics and Mechatronics Lab at Virginia Tech, Anil Kumar for his help on the electrical design and Peter Racioppo his help in static and dynamic analysis.

REFERENCES

[1] P. M. Moubarak and P. Ben-Tzvi, "A Tristate Rigid Reversible and Non-Back-Drivable Active Docking Mechanism for Modular Robotics," *IEEE/ASME Trans. Mechatronics*, vol. 19, no. 3, pp. 840–851, 2014.

[2] M. Yim, W. M. Shen, B. Salemi, D. Rus, M. Moll, H. Lipson, E. Klavins, and G. S. Chirikjian, "Modular self-reconfigurable robot systems [Grand challenges of robotics]," *IEEE Robot. Autom. Mag.*, vol. 14, no. 1, pp. 43–52, 2007.

[3] M. Yim, Y. Zhang, and D. Duff, "Modular robots," *IEEE Spectr.*, vol. 39, no. 2, pp. 30–34, 2002.

[4] P. Ben-Tzvi, A. A. Goldenberg, and J. W. Zu, "Articulated hybrid mobile robot mechanism with compounded mobility and manipulation and on-board wireless sensor/actuator control interfaces," *Mechatronics*, vol. 20, no. 6, pp. 627–639, Sep. 2010.

[5] W. Saab and P. Ben-Tzvi, "A Genderless Coupling Mechanism with 6-DOF Misalignment Capability for Modular Self-Reconfigurable Robots," *J. Mech. Robot.*, vol. 8, no. c, pp. 1–9, 2016.

[6] P. Ben-Tzvi, "Experimental validation and field performance metrics of a hybrid mobile robot mechanism," *J. F. Robot.*, vol. 7, no. PART 1, 2010.

[7] P. Moubarak and P. Ben-Tzvi, "Modular and reconfigurable mobile robotics," *Rob. Auton. Syst.*, vol. 60, no. 12, pp. 1648–1663, 2012.

[8] M. Park, S. Chitta, a. Teichman, and M. Yim, "Automatic Configuration Recognition Methods in Modular Robots," *Int. J. Rob. Res.*, vol. 27, no. 3–4, pp. 403–421, 2008.

[9] W. Wang, W. Yu, and H. Zhang, "JL-2: A mobile multi-robot system with docking and manipulating capabilities," *Int. J. Adv. Robot. Syst.*, vol. 7, no. 1, pp. 9–18, 2010.

[10] O. Purwin and R. D'Andrea, "Trajectory generation and control for four wheeled omnidirectional vehicles," *Rob. Auton. Syst.*, vol. 54, no. 1, pp. 13–22, 2006.

[11] J. Sastra, S. Chitta, and M. Yim, "Dynamic Rolling for a Modular Loop Robot," *Int. J. Rob. Res.*, vol. 28, no. 6, pp. 758–773, 2009.

[12] W. M. Shen, H. C. H. Chiu, M. Rubenstein, and B. Salemi, "Rolling and climbing by the multifunctional SuperBot reconfigurable robotic system," *AIP Conf. Proc.*, vol. 969, pp. 839–848, 2008.

[13] A. Kamimura, H. Kurokawa, E. Yoshida, S. Murata, K. Tomita, and S. Kokaji, "Automatic locomotion design and experiments for a modular robotic system," *IEEE/ASME Trans. Mechatronics*, vol. 10, no. 3, pp. 314–325, 2005.

[14] F. Mondada, M. Bonani, A. Guignard, S. Magnenat, C. Studer, and D. Floreano, "Superlinear physical performances in a swarm-bot," *Lect. Notes Comput. Sci. (including Subser. Lect. Notes Artif. Intell. Lect. Notes Bioinformatics)*, vol. 3630 LNAI, pp. 282–291, 2005.

[15] Dazhai Li, Hualei Fu, and Wei Wang, "Ultrasonic based autonomous docking on plane for mobile robot," in *2008 IEEE International Conference on Automation and Logistics*, 2008, no. September, pp. 1396–1401.

[16] H. B. Brown, J. M. Vande Weghe, C. A. Bererton, and P. K. Khosla, "Millibot trains for enhanced mobility," *IEEE/ASME Trans. Mechatronics*, vol. 7, no. 4, pp. 452–461, Dec. 2002.

[17] B. Li, S. Ma, J. Liu, M. Wang, T. Liu, and Y. Wang, "AMOEBA-I: A Shape-Shifting Modular Robot for Urban Search and Rescue," *Adv. Robot.*, vol. 23, no. 9, pp. 1057–1083, 2009.

[18] G. J. Hamlin and a. C. Sanderson, "TETROBOT modular robotics: prototype and experiments," *Proc. IEEE/RSJ Int. Conf. Intell. Robot. Syst. IROS '96*, vol. 2, pp. 390–395, 1996.

[19] G. G. Ryland and H. H. Cheng, "Design of iMobot, an intelligent reconfigurable mobile robot with novel locomotion," in *2010 IEEE International Conference on Robotics and Automation*, 2010, pp. 60–65.

[20] M. Yim, D. G. Duff, and K. D. Roufas, "PolyBot: a modular reconfigurable robot," *Proc. 2000 ICRA. Millenn. Conf. IEEE Int. Conf. Robot. Autom. Symp. Proc. (Cat. No.00CH37065)*, vol. 1, no. April, pp. 514–520, 2000.

[21] H. Zhang, J. Gonzalez-Gomez, Z. Xie, S. Cheng, and J. Zhang, "Development of a low-cost flexible modular robot GZ-I," *IEEE/ASME Int. Conf. Adv. Intell. Mechatronics, AIM*, pp. 223–

228, 2008.
[22] M. C. Shiu, H. T. Lee, F. L. Lian, and L. C. Fu, *Design of the Octabot self-reconfigurable robot*, vol. 17, no. 1 IFAC, 2008.
[23] A. Lyder, R. F. M. Garcia, and K. Stoy, "Mechanical design of Odin, an extendable heterogeneous deformable modular robot," in *2008 IEEE/RSJ International Conference on Intelligent Robots and Systems, IROS*, 2008, pp. 883–888.
[24] C. Unsal, H. Kiliccote, and P. K. Khosla, "I(CES)-cubes: a modular self-reconfigurable bipartite robotic system," in *Sensor Fusion and Decentralized Control in Robotic Systems II*, 1999, vol. 3839, no. September, pp. 258–269.
[25] A. Spröwitz, S. Pouya, S. Bonardi, J. Van Den Kieboom, R. Möckel, A. Billard, P. Dillenbourg, and A. Ijspeert, "Roombots: Reconfigurable robots for adaptive furniture," *IEEE Comput. Intell. Mag.*, vol. 5, no. 3, pp. 20–32, 2010.
[26] V. Zykov, A. Chan, and H. Lipson, "Molecubes: An Open-Source Modular Robotics Kit," *IROS-2007 Self-Reconfigurable Robot. Work.*, pp. 3–6, 2007.
[27] A. Kawakami, A. Torii, K. Motomura, and S. Hirose, "SMC Rover: Planetary Rover with transformable wheels," *Exp. Robot. VIII*, vol. 5, pp. 498–506, 2003.
[28] A. Castano, A. Behar, and P. M. Will, "The Conro modules for reconfigurable robots," *IEEE/ASME Trans. Mechatronics*, vol. 7, no. 4, pp. 403–409, 2002.
[29] N. S. Flann and K. L. Moore, "A six-wheeled omnidirectional autonomous mobile robot," *IEEE Control Syst. Mag.*, vol. 20, no. 6, pp. 53–66, 2000.
[30] G. Indiveri, "Swedish wheeled omnidirectional mobile robots: Kinematics analysis and control," *IEEE Trans. Robot.*, vol. 25, no. 1, pp. 164–171, Feb. 2009.
[31] G. Bayar, B. A. Koku, and E. I. Konukseven, "Design of a configurable all terrain mobile robot platform," *Int. J. Math. Model. Methods Appl. Sci.*, vol. 3, no. 4, pp. 366–373, 2009.
[32] J. Kim, Y. Kim, and J. Kwak, "Wheel & Track hybrid robot platform for optimal navigation in an urban environment," in *SICE Annual Conference …*, 2010, pp. 881–884.
[33] Z. Li, S. Ma, B. Li, M. Wang, and Y. Wang, "Parameter design and optimization for mobile mechanism of a transformable wheel-track robot," in *2009 IEEE International Conference on Automation and Logistics*, 2009, no. August, pp. 158–163.
[34] F. Michaud, D. Létourneau, M. Arsenault, Y. Bergeron, R. Cadrin, F. Gagnon, M. A. Legault, M. Millette, J. F. Paré, M. C. Tremblay, P. Lepage, Y. Morin, J. Bisson, and S. Caron, "Multi-modal locomotion robotic platform using leg-track-wheel articulations," *Auton. Robots*, vol. 18, no. 2, pp. 137–156, 2005.
[35] K. J. Huang, S. C. Chen, Y. C. Chou, S. Y. Shen, C. H. Li, and P. C. Lin, "Experimental validation of a leg-wheel hybrid mobile robot quattroped," in *Proceedings - IEEE International Conference on Robotics and Automation*, 2011, pp. 2976–2977.
[36] S. Y. Shen, C. H. Li, C. C. Cheng, J. C. Lu, S. F. Wang, and P. C. Lin, "Design of a leg-wheel hybrid mobile platform," *2009 IEEE/RSJ Int. Conf. Intell. Robot. Syst. IROS 2009*, pp. 4682–4687, 2009.
[37] Hyok-Jo Kwon, Hyungwon Shim, Doo-Gyu Kim, Sung-Kook Park, and Jihong Lee, "A development of a transformable caterpillar equipped mobile robot," in *2007 International Conference on Control, Automation and Systems*, 2007, pp. 1062–1065.
[38] "Wheelchair, GALILEO." [Online]. Available: http://www.youtube.com/watch?v=AZ9DotVwhlQ. [Accessed: 09-Feb-2017].
[39] A. Weiss, R. G. Langlois, and M. J. D. Hayes, "Unified treatment of the kinematic interface between a sphere and omnidirectional wheel actuators," *J. Mech. Robot.*, vol. 3, no. 4, p. 41001, 2011.
[40] M. Udengaard and K. Iagnemma, "Analysis, Design, and Control of an Omnidirectional Mobile Robot in Rough Terrain," *J. Mech. Des.*, vol. 131, no. 12, p. 121002, 2009.
[41] S. Ostrovskaya, "Dynamics of a Mobile Robot with Three Ball-Wheels," *Int. J. Rob. Res.*, vol. 19, no. 4, pp. 383–393, 2000.
[42] J. E. Mohd Salih, M. Rizon, and S. Yaacob, "Designing Omni-Directional Mobile Robot with Mecanum Wheel," *Am. J. Appl. Sci.*, vol. 3, no. 5, pp. 1831–1835, 2006.
[43] R. L. Williams, B. E. Carter, P. Gallina, and G. Rosati, "Dynamic model with slip for wheeled omnidirectional robots," *IEEE Trans. Robot. Autom.*, vol. 18, no. 3, pp. 285–293, 2002.
[44] K. Tadakuma, R. Tadakuma, and J. Berengeres, "Development of holonomic omnidirectional vehicle with 'Omni- Ball': Spherical wheels," *IEEE Int. Conf. Intell. Robot. Syst.*, pp. 33–39, 2007.
[45] J. H. Lee, B. K. Kim, T. Tanikawa, and K. Ohba, "Kinematic analysis on omni-directional mobile robot with double-wheel-type active casters," *ICCAS 2007 - Int. Conf. Control. Autom. Syst.*, pp. 1217–1221, 2007.
[46] I. Doroftei, V. Grosu, and V. Spinu, *Omnidirectional Mobile Robot – Design and Implementation*, no. September. 2007.
[47] K. Tadakuma, R. Tadakuma, A. Maruyama, E. Rohmer, K. Nagatani, K. Yoshida, Aigo Ming, M. Shimojo, M. Higashimori, and M. Kaneko, "Mechanical design of the Wheel-Leg hybrid mobile robot to realize a large wheel diameter," in *2010 IEEE/RSJ International Conference on Intelligent Robots and Systems*, 2010, vol. 1, pp. 3358–3365.
[48] W. Saab and P. Ben-Tzvi, "Development of a Novel Coupling Mechanism for Modular Self-Reconfigurable Mobile Robots," in *Volume 5B: 39th Mechanisms and Robotics Conference*, 2015, p. V05BT08A007.
[49] D. P. Miller, Li Tan, and S. Swindell, "Simplified navigation and traverse planning for a long-range planetary rover," in *2003 IEEE International Conference on Robotics and Automation (Cat. No.03CH37422)*, 2003, pp. 2436–2441.
[50] T. Kubota, Y. Kuroda, Y. Kunii, and I. Nakatani, "Small, light-weight rover 'Micro5' for lunar exploration," *Acta Astronaut.*, vol. 52, no. 2–6, pp. 447–453, 2003.
[51] "iRobot PackBot." [Online]. Available: http://www.army-technology.com/projects/irobot-510-packbot-multi-mission-robot/. [Accessed: 09-Feb-2017].
[52] "Seegrid Trucks." [Online]. Available: http://www.cisco-eagle.com/catalog/c-4173-robotic-industrial-trucks.aspx. [Accessed: 09-Feb-2017].
[53] U. Saranli, M. Buehler, and D. E. Koditschek, "RHex: A Simple and Highly Mobile Hexapod Robot," *Int. J. Rob. Res.*, vol. 20, no. July, pp. 616–631, 2001.
[54] M. Raibert, "BigDog, the rough-terrain quadruped robot," *IFAC Proc. Vol.*, vol. 17, no. 1 PART 1, pp. 6–9, 2008.
[55] F. Michaud, M. Arsenault, Y. Bergeron, R. Cadrin, F. Gagnon, M.-A. Legault, M. Millette, J.-F. Paré, M.-C. Tremblay, D. Létourneau, P. Lepage, Y. Morin, S. Caron, and J. Bisson, "Co-Design of AZIMUT: A Multi-Modal Robotic Platform," in *Volume 1: 23rd Computers and Information in Engineering Conference, Parts A and B*, 2003, vol. 2003, pp. 801–810.
[56] Ben-Tzvi, P., Moubarak, P., "A mobile Robot with Hybrid Traction and Mobility Mechanism", U.S. Patent 9,004,200, Issued April 14, 2015.
[57] Ben-Tzvi, P., Moubarak, P., "Active Docking Mechanism for Modular and Reconfigurable Robots", U.S. Patent 9,616,948, Issued April 11, 2017.

